Science of the Total Environment 753 (2021) 141950

Contents lists available at ScienceDirect

Science of the Total Environment

journal homepage: www.elsevier.com/locate/scitotenv

Highly specific nanobody against herbicide 2,4-dichlorophenoxyacetic acid for monitoring of its contamination in environmental water

Zhen-Feng Li [a,e], Jie-Xian Dong [a,e], Natalia Vasylieva [a], Yong-Liang Cui [b], De-Bin Wan [a], Xiu-De Hua [c], Jing-Qian Huo [d], Dong-Chen Yang [d], Shirley J. Gee [a], Bruce D. Hammock [a,*]

[a] Department of Entomology and UCD Comprehensive Cancer Center, University of California, Davis, California 95616, United States
[b] Ministry of Agriculture, Citrus Research Institute, Southwest University, Chongqing 400712, PR China.
[c] College of Plant Protection, Nanjing Agricultural University, Nanjing 210095, PR China
[d] College of Plant Protection, Agricultural University of Hebei, Baoding 071001, PR China
[e] Guangzhou Nabo Antibody Technology Co. Ltd, Guangzhou 510530, PR China

HIGHLIGHTS

- Reliable step-wise workflow for anti-hapten nanobody discovery was presented.
- Highly specific and sensitive nanobody against 2,4-D was obtained by optimized isolation procedure.
- A sensitive one-step FLEIA for 2,4-D was developed based on nanobody-AP fusion protein.
- The assay showed to be useful and applicable for monitoring 2,4-D pollution in environmental water.

GRAPHICAL ABSTRACT

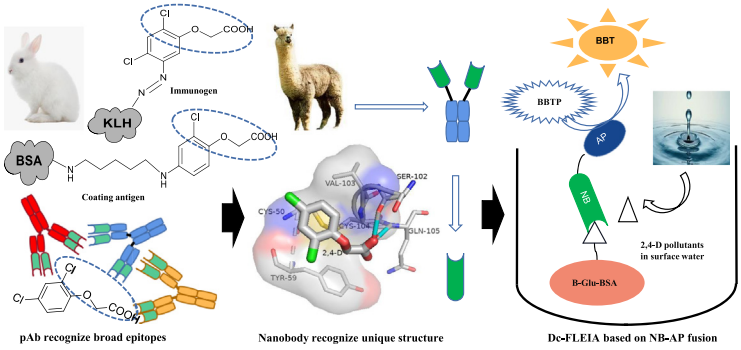

ARTICLE INFO

Article history:
Received 15 July 2020
Received in revised form 22 August 2020
Accepted 22 August 2020
Available online 24 August 2020

Editor: Damia Barcelo

Keywords:
Surface water monitoring
Antibody specificity
Nanobody isolation
FLEIA based on nanobody-AP

ABSTRACT

2,4-dichlorophenoxyacetic acid (2,4-D), a widely used herbicide, is a small organic chemical pollutant in the environment. To develop a nanobody-based immunoassay for monitoring trace levels of 2,4-D, a step-wise strategy for the generation of nanobodies highly specific against this small chemical was employed. Firstly, we synthesized three novel haptens mimicking 2,4-D and assessed their influence on the sensitivity and specificity of the existing antibody-based assay. Polyclonal antibodies (pAb) from rabbits showed good sensitivity and moderate specificity for 2,4-D, pAb from llama based on selected haptens showed similar performance when compared to those from rabbits. Secondly, nanobodies derived from llama were generated for 2,4-D by an effective procedure, including serum monitoring and one-step library construction. One nanobody, NB3-9, exhibited good sensitivity against 2,4-D (IC_{50} = 29.2 ng/mL) had better specificity than the rabbit pAb#1518, with no cross-reactivities against the 2,4-D analogs tested. Thirdly, one-step fluorescent enzyme immunoassay (FLEIA) for 2,4-D based on a nanobody-alkaline phosphatase (AP) fusion was developed with IC_{50} of 1.9 ng/mL and a linear range of 0.4–8.6 ng/mL. Environmental water samples were analyzed by FLEIA and LC-MS/MS for comparison, and the results were consistent between both methods. Therefore, the proposed step-wise strategy from hapten design to nanobody-AP fusion production was successfully conducted, and the resulting nanobody based FLEIA was demonstrated as a convenient tool to monitor 2,4-D residuals in the environment.

* Corresponding author.
E-mail address: bdhammock@ucdavis.edu (B.D. Hammock).

https://doi.org/10.1016/j.scitotenv.2020.141950
0048-9697/

1. Introduction

2,4-Dichlorophenoxyacetic acid (2,4-D) is one of the chlorophenoxy herbicides, most frequently used in agriculture and forestry (Burns and Swaen, 2012). Recently, Dow Agro-Sciences developed 2,4-D-resistant crops which were approved by the U.S. Department of Agriculture (Egan et al., 2011). Thus, it is predicted that the use of 2,4-D will greatly increase in the near future. Since the widespread use of 2,4-D causes concern over environmental contamination (Teixeira et al., 2007) and possibly human health (Zuanazzi et al., 2020), the pollution of 2,4-D in environmental water is attracting more attention. Several immunoassays (Kaur et al., 2008) and immunosensor assays (Feng et al., 2017) have been developed for detection of 2,4-D because they are cost-effective and rapid compared with the traditional chromatography methods(Mohammadnia et al., 2019).

A key criterion of immunoassays for the detection of small chemicals is the use of highly selective antibodies without obvious cross-reactivity to other similar chemicals. However, the reported polyclonal and monoclonal antibodies against 2,4-D were raised by a traditional strategy of preparing immunogens and coating antigens (Franek et al., 1994), which were coupled to carried proteins via the carboxyl group in 2,4-D. This procedure hides the carboxyl group as a recognition element for potential antibodies. Consequently, the reported 2,4-D antibodies exhibited high cross-reactivity with other herbicides like 2,4-D ester derivatives (Franek et al., 1994), MCPA(Gerdes et al., 1997), 2,4-dichlorophenoxybutyric acid(Kaur et al., 2008), and dichlorprop (Matuszczyk et al., 1996), these chlorophenoxy herbicides usually occurred in the same circumstance (Gamhewage et al., 2019; Seebunrueng et al., 2020). High cross-reactivity with other herbicides is the undesired characteristic of existing immunoassays for the detection of 2,4-D. Apparently, all published immunochemical analysis mentioned above is not specialized for the detection of 2,4-D,because it is hard to distinguish 2,4-D along from the interference from other chemically similar herbicides. To overcome this limitation, novel design and synthesis of haptens for the generation of antibodies against 2,4-D need to be considered. Generally, to generate highly selective antibodies against small chemicals, the mimicking haptens are synthesized with different functional groups for conjugation with protein and keep the most prominent group exposed for the immune response (Mi et al., 2019; Mu et al., 2014). Besides, the conjugation site, linker type, and length between hapten and carrier protein have been investigated (Cevallos-Cedeno et al., 2018; Mi et al., 2019). Most of the 2,4-D analogs have similar chemical structures, and all of them shared the common chlorophenoxy structure. The carboxyl group attached to chrolophenxy group seems to be a unique structural feature of 2,4-D. Thus, the exposure of this epitope in 2,4-D hapten design is important for specific immune reaction in immunization to generate a high specific antibody distinguishing 2,4-D and other chrolophenxy herbicides. In this study, 2,4-D also serves as a model small chemical target. Using it, the serum response toward different haptens will be assessed, and the relationship between hapten design and antibody specificity will be investigated as described below.

Recently, a type of recombinant antibody, colloquially named nanobodies, has become a powerful reagent for immunoassay applications (Hassanzadeh-Ghassabeh et al., 2013; He et al., 2018). In the past few years, our laboratory had reported multiple nanobodies against small molecules (Bever et al., 2016), like 3-PBA (Kim et al., 2012), TBBPA (Wang et al., 2014). etc. However, considering the tiny epitope of small molecule, the critical factors to produce a nanobody with high sensitivity and specificity are not established and remain controversial. One uncertain factor for nanobody isolation from llama is the amount of heavy chain-only antibodies contained in the serum of llama after the cycles of immunization (Tabares-da Rosa et al., 2011). The heavy chain only antibodies (named as IgG2 and IgG3) were considered as the original source of nanobodies (Hamers-Casterman et al., 1993), therefore, to confirm the existence of subclass IgG2 + 3 after the immunization period is a critical step before nanobody library construction (Tillib et al., 2014). Another uncertain factor for nanobody isolation from llama is how to assure and enhance the diversity of nanobody library construction. There are many reported strategies to amplify the nanobody repertoire by PCR from peripheral blood mononuclear cells (PBMCs). Unlike traditional two-step nest PCR strategies, one-step PCR directly amplifies all the IgG2 and IgG3 isotypes (Pardon et al., 2014). The one-step PCR strategy is believed to maintain the diversity of the nanobody repertoire, including all heavy chain only antibody isotypes (Kastelic et al., 2009; van der Linden et al., 2000), which is critical for isolation a nanobody with excellent specificity and sensitivity.

In this study, 2,4-D was chosen as a model target to demonstrate how to develop an immunoassay against chemical pollutants with desired sensitivity and excellent specificity. We performed a stepwise procedure to refine the generation of nanobodies with several critical steps, including hapten design, rabbit/llama antiserum assessment, and one-step library construction. Further, the high specific nanobody against 2,4-D was fused to alkaline phosphatase (AP) for the development of one-step fluorescence enzyme immunoassay (FLEIA). This sensitive immunoassay based on nanobody-AP fusion was applied to monitor the 2,4-D contamination in environmental water.

2. Materials and methods

The detailed description of information about chemicals, reagents, instruments and the entire procedure of workflow from hapten design to nanobody isolation and nanobody-AP fusion preparation is listed in the supporting information.

2.1. Synthesis of haptens and preparation of immunogen and coating antigens

Three haptens showed in Fig. 1 were obtained by introducing an amino or sulfhydryl group in different sites of the 2,4-D molecule, and the experiment detail are described in supporting information 2.1. The conjugations of three haptens with carrier proteins are also described in supporting information2.2. **Hapten A and Hapten B** were coupled to carrier proteins (BSA or KLH) using the diazotization reaction or glutaraldehyde reactions (Fig. S1). **Hapten C** was conjugated to carrier proteins (BSA or KLH) by the heterobifunctional agent 3-(2-pyridyldithio) propionic acid N-hydroxy succinimide ester (SPDP).

2.2. Immunization and antiserum assessment

Five immunogens were used to produce the pAbs, respectively, following the standard rabbit immunization procedure (supporting information 3.1). An indirect competitive ELISA(ic-ELISA) procedure was developed for rabbit serum assessment (supporting information 3.2). The selected immunogen was used in the following llama immunization procedure. The titer of the successive bleeds of llama serum against different coating antigens were also determined by ELISA (supporting information 3.3/3.4). Llama IgG isotypes from the final bleed were obtained by protein A&G column separation and analyzed by reduced SDS-PAGE (Fig. S2). The experiment details are described in supporting information 3.3.

2.3. Library construction, biopanning and screening the nanobody

First step of the library construction procedure is the same as the routine protocol from total mRNA extraction to RT-PCR synthesis of cDNA. DNA fragments encoding different subclass heavy chain IgG variable domains (nanobody gene) were obtained by PCR amplification with a set of primers (Table S1). The library construction and biopanning procedure were described in supporting information 4.1. Almost 100 individual

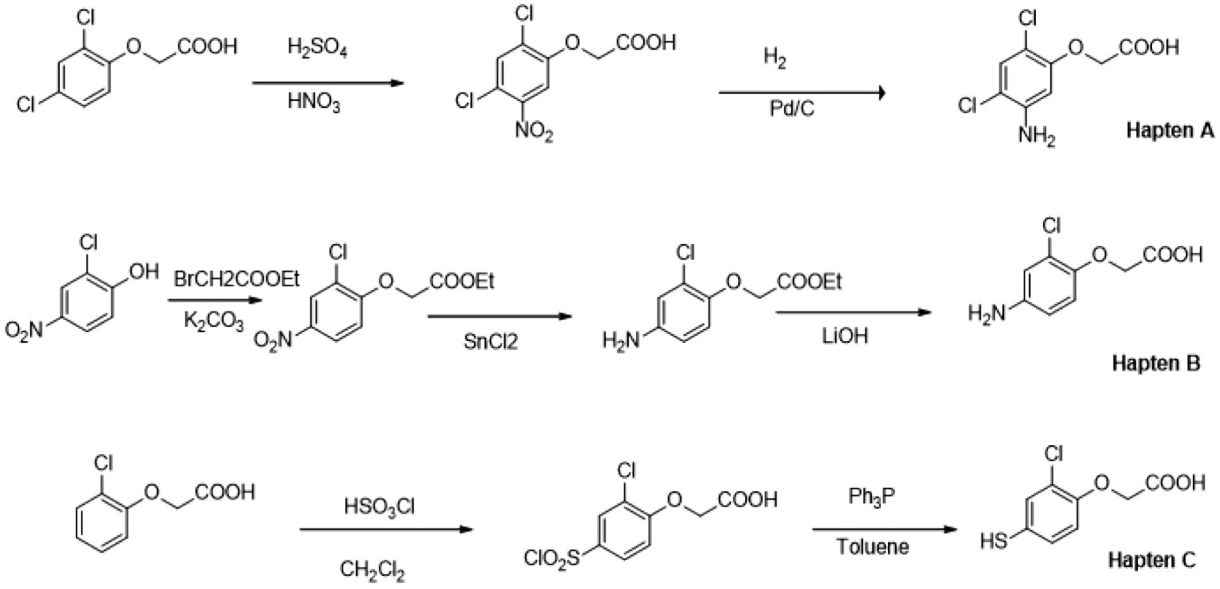

Fig. 1. Synthesis approach of haptens with different functional groups located at different site of benzene ring.

clones from the last round were selected for screening by ELISA in nanobody-G3 fusion format (supporting information 4.2). The positive nanobody candidates were expressed in pET28 vector, purified, and further analyzed by ic-ELISA (supporting information 4.3).

2.4. Specificity of antibodies against 2,4-D and computer simulation analysis

Two ic-ELISA procedures were developed to assess the sensitivity of pAb and isolated nanobodies in the previous sections (supporting information 3.2/4.3). Then, the selectivity of pAb and best nanobody were evaluated by testing the cross-reactivity (CR) of a set of 2,4-D structural analogs. The relative CR was calculated by the following formula: CR (%) = $[IC_{50}(2,4\text{-D})/IC_{50}(\text{tested compound})] \times 100$. To understand the CR of nanobody against 2,4,-D and its analogs, the recognition mechanism between nanobody and 2,4-D was further analyzed by a simulation docking study. First, the 3D model of nanobody was constructed by homogenous modeling in YASARA (Krieger et al., 2002). The nanobody 3D model was evaluated using PROCHECK (Laskowski et al., 1993), and then the 3D structure of 2,4-D was docked to the binding site of nanobody model by AutoDockLGA (Forli et al., 2016). The binding energy and dissociation constants were calculated, and the inter-molecule interactions between the critical residues of nanobody and functional group on 2,4-D are presented in visualization format. All stimulation experiment detail are described in supporting information 4.4.

2.5. Preparation of nanobody-AP fusion and development of FLEIA/ELISA

The plasmids containing the best nanobody were amplified with primers (Table S1), and ligated to expression plasmid containing the AP gene followed by transformation into cells of *E.coli*. The expression and purification of nanobody-AP fusion were conducted following the protocol described in supporting information 5.1. The development of one-step FLEIA/ELISA based on nanobody-AP was conducted as described in supporting information 5.2. The matrix effect of water sample was investigated by dilution of the water sample with PBS assay buffer. To check the accuracy of the developed FLEIA, the water samples spiked with 2,4-D were analyzed for recovery study and the real water samples were detected by both FLEIA and HPLC-MS/MS analysis (supporting information 5.3).

3. Results and discussion

3.1. Hapten design and polyclonal antibody performance

2,4-D, a small organic molecule as an herbicide, has a carboxyl group in its chemical structure (Fig. 1). Many research groups used the carboxyl group as a simple way to conjugate 2,4-D with a carrier protein to produce antibodies. Although this method requires no synthetic chemistry, it has some limitations. Coupling the proteins from the carboxyl group lead to antibodies that had poor specificity against 2,4-D, because corresponding antibodies mainly recognize the 2,4-dichlorobenzene part of 2,4-D, which is a common structure in many 2,4-D analogs (Kaur et al., 2008). To distinguish 2,4-D from other dichlorobenzene herbicides, particularly the related esters, the unique carboxyl functional group should be retained in hapten design. Based on this consideration, three novel haptens of 2,4-D were designed and synthesized. The haptens had either an amino or sulfhydryl group, distal to the carboxyl group, so that the carboxyl group was exposed on the surface of carrier protein after conjugation. According to the procedure in Fig. 1, three haptens were successfully synthesized. Hapten A/B had the functional amine group in different sites of the benzene ring for conjugation. Hapten A retained both chlorine groups, while the Hapten B only retained one chlorine groups. The Hapten C was designed similarly as hapten B with a minor substitution from the amino group to a sulfhydryl group for conjugation. Here we applied two methods, diazotization and glutaraldehyde reactions, for the conjugation of hapten A/B with carrier protein for immunogen and coating antigen (Fig. S1). The diazotization method formed an azo group between 2,4-D hapten and the carrier protein, which helps the hapten expose on the surface of a carrier protein in a rigid manner. In contrast, the glutaraldehyde (Glu) introduced a flexible six atoms linker between hapten and the carrier protein. In addition, hapten C was coupled with carrier proteins (BSA or KLH) by the heterobifunctional agent 3-(2-pyridyldithio) propionic acid N-hydroxysuccinimide ester (SPDP). SPDP, as a long linker, also increased distance between 2,4-D hapten and carrier protein.

All of the 5 sera from immunized rabbits were screened against five coating antigens using checkerboard titration. Anti-serum #1519 obtained through immunization with A-Glu-KLH and #1521 with B-Glu-KLH had no or low titer to all the coating antigens. The same

phenomenon happened to rabbit #1522, where the immunogen was C-SPDP-KLH. Rabbits #1518, #1520 immunized with A/B-Dia-KLH had high titers to coating antigens B-Glu-BSA and C-SPDP-BSA, and they had no or low titer to other coating antigens (Table 1). The immunogen containing the Glu and SPDP linker gave a poor immunization response. We assumed that the rigid hapten with no linker is more stable when exhibiting on the carrier protein, it could cause a long-term simulation during immunization. Alternatively, the hapten with longer linker is flexible when attached on the surface of carrier protein, so it is hard to maintain a strong immuno simulation. As shown in Table 1, most of the antiserum have better response versus their corresponding homologous coating antigen than the heterologous coating antigen. However, the B-Glu-BSA as heterologous coating antigen have better signal with antiserum#1518 than the homologous coating antigen A-Dia-BSA Same phenomenon we also observed in another long linker SPDP. The C-SPDP-BSA as heterologous coating antigen also have better signal with antiserum#1518, #1520 and #1521 than their homologous immunogen. The major reason for higher signal from some antiserum versus their corresponding homologous or heterologous coating antigen is the inconsistent conjugate efficiency. In addition, we speculated that longer linkers (Glu and SPDP) made the hapten easily exposure on the surface of carrier protein, which benefit the antigen-antibody binding during the immunoassay. In our study, the most suitable antiserum was obtained from the immunogen with the short linker and coating antigen containing a longer linker. After optimization, serum#1518 from A-Dia-KLH immunogen was selected to develop a competitive assay in heterologous format combined with the B-Glu-BSA as coating antigen, the IC_{50} of standard curve against 2,4-D was 2.4 ng/mL (Fig. 2a). This developed ELISA was applied to check the cross-reactivity of an obtained pAb#1518 for the analogs of 2,4-D (Table 2). We hypothesized that haptens that conserve the carboxylic acid group would result in antibodies that would not recognize or recognized less the corresponding methyl or butyl esters. Although our pAb#1518 obtained with new hapten showed some cross-reactivity to the methyl ester (about 35%), this was much lower than that obtained by the previously reported antibodies(Franek et al., 1994; Lawruk et al., 1994) immunized with carboxyl group derived hapten (945% for rabbit polyclonal antibodies in Lawruk's work) or (71–160% for 12 monoclonal antibodies in Franek 's work). Similarly, our assay cross-reacted with 2,4-D butyl ester about 35%, while the Lawruk's assay cross-reacted 646% (Lawruk et al., 1994). Chlorine on the ring is also important for recognition since phenoxy acetic acid did not cross-react. In addition, substituting $-CH_3$ (2,4-dichlorotoluene) or –OH (2,4,5-trichlorophenol) for the acetic acid also resulted in no binding. Unexpectedly, the pAb#1518 still has cross-reactivity against other herbicides like MCPA, dichlorprop, fenoprop, which all contain the carboxyl group in their molecular structure. Moreover, 2,4,5-T was characterized by the highest percent of cross-reactivity (156.6%), likely because it was structurally similar to 2,4-D except for extra chlorine on the benzene ring. It indicated the pAb#1518 raised thorough optimized hapten design still recognizes the broad epitopes, including not only the carboxyl group but also the chlorophenoxy group of 2,4-D. The cross-reactivity could lead to false-positive results if these 2,4-D esters and analogs are present in the same circumstance. The pAb#1518 obtained in our study actually was a mixture of antibodies against different structure epitopes of 2,4-D, so it is hard to optimize the specificity of pAb. Therefore, we pursued an approach toward single-domain, small variable antibody fragments engineered from the camelid IgG family, called "nanobodies" (Khodabakhsh et al., 2018), as an alternative to the pAb. This single epitope-specific binder has a different binding pattern compared with classic IgG (Togtema et al., 2019), which might have the potency to recognize the unique chemical structure on 2,4-D.

3.2. Serum response of llama immunization

One llama was immunized with the selected immunogen as described earlier. After the boost, serum from several cycles of immunizations was collected, the 3rd, 5th, and 7th bleeds from immunized llama were analyzed by ELISA against different coating antigens. As shown in Table 1, llama immunized with A-Dia-KLH, showed response with different coating antigens. The best binding was with the coating antigen containing the longer linker, like B-Glu-BSA and C-SPDP-BSA. The immune response that occurred in llama was consistent with the response that happened in the rabbit. In addition, the immune response occurred faster in rabbit than llama in our study, Therefore, screening hapten design in rabbits and transferring to llamas is an efficient approach for reducing time and cost at assay development.

It is well known that llamas produce not only conventional IgG1 but also functional IgG isotypes that do not incorporate light chains. These heavy-chain only IgG isotypes are usually classified as IgG2 and IgG3 (Fig. S2). Since nanobodies are derived from the heavy chain antibody, it is critical to identify the existence of IgG2 and IgG3 in the whole population of llama serum. The IgG subclasses in the last bleeding of llama were separated using the protein G and protein A procedure (Fig. S2). As shown in the reduced SDS-PAGE analysis, each subclass of IgG with their characteristic band features were obtained: IgG1 had a heavy chain (50 kDa) and light chain (25 kDa), while IgG2 and IgG3 only had the heavy chain (40–45 kDa). Though the band of IgG3 was weak, the band of IgG2 was stronger than the IgG1; this means that more of the heavy chain IgG only fraction existed in the whole antibody population. Based on these results, we were convinced that after 7 rounds of immunization, it was time to collect the PBMCs for the next step of library construction.

3.3. One-step variable domain library construction and isolation of nanobodies

For library construction, total RNA was extracted from the PBMC of llama and reverse transcribed to cDNA according to the routine protocol of our laboratory (Kim et al., 2012). The next step is the amplification of variable gene encoded nanobody from cDNA to construct the nanobody library. Usually, the gene encoding nanobody form FR1 to FR4 region was amplified in complicated two-step nested PCR strategy (Arbabi Ghahroudi et al., 1997). However, some researchers reported that the genetic diversity of nanobody repertoire could get lost in this two-step PCR due to PCR bias (Kastelic et al., 2009). Recently, some research

Table 1
Antiserum titer response of rabbits/llama against coating antigens.

Coating Antigens	Final rabbit serum by different immunogens					llama immunized with A-Dia-KLH		
	A-Dia-KLH (#1518)	A-Glu-KLH (#1519)	B-Dia-KLH (#1520)	B-Glu-KLH (#1521)	C-SPDP-KLH (#1522)	3rd bleed	5th bleed	7th bleed
A-Dia-BSA	+	+	+	+	−	+	++	++
A-Glu-BSA	−	+	−	−	−	−	+	+
B-Dia-BSA	−	−	+	−	−	−	+	+
B-Glu-BSA	+++	−	+++	++	−	+++	++++	++++
C-SPDP-BSA	+++	−	+++	+++	+	+++	++++	++++

[a]The data shown were at a coating antigen concentration of 1 μg/mL and an antibody dilution of 1:1000; −, absorbance <0.3; +, absorbance 0.3–0.6; ++, absorbance 0.6–0.9; +++, absorbance 0.9–1.2; and ++++, absorbance >1.2.

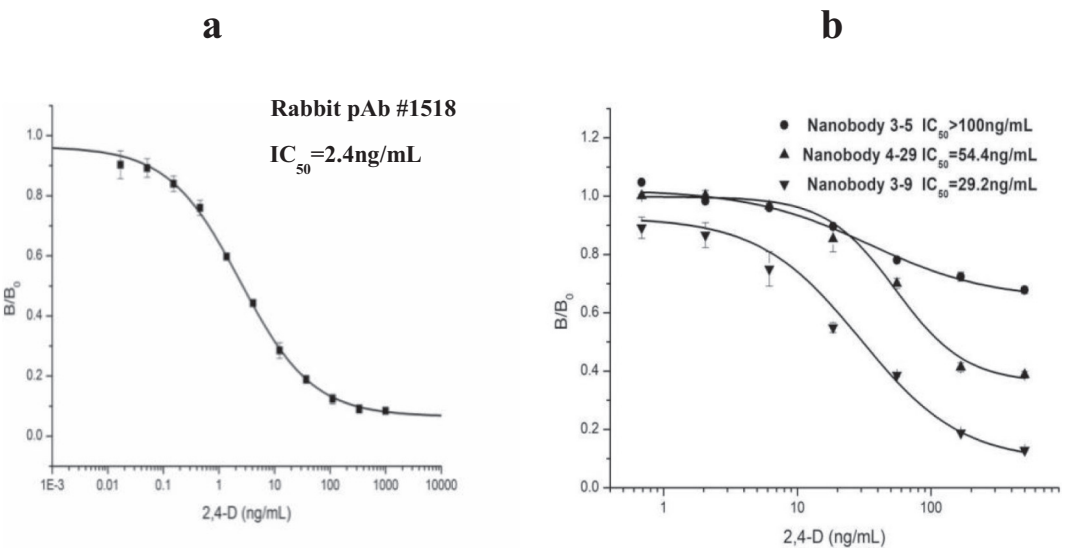

Fig. 2. Standard curve of ic-ELISA based on rabbit pAb#1518 (a) and isolated nanobodies (b).

discovered that the nanobody gene is different from the traditional heavy chain gene in the hinge region (Daley et al., 2005), and many isotypes of nanobody subclass have been identified as IgG2a/b/c and IgG3(Griffin et al., 2014; Tillib et al., 2014). Thus, a simple one-step PCR strategy was proposed in our study for cloning the variable gene of different IgG isotypes directly (Fig. 3). Using the primer listed in Table S1, the nanobody gene in 4 subclasses was amplified from FR1 to the upper hinge region, and then the resulting nanobody repertoire was directly cloned to the pComb3X vector for library construction. The phage-displayed nanobody library with a size of 3.4×10^7 clones was bio-panned in three rounds against the selected coating antigen B-Glu-BSA. To isolate a nanobody with desirable specificity, all-rounds of panning were performed in competitive mode. Successive decreasing the concentration of the free 2,4-D in three rounds served as a stringent bio-panning strategy to obtain the phage-displayed nanobody binding selectively against 2,4-D. Selected clones from the last round were expressed in a deep well culture plate, then the binding capacity and the 2,4-D inhibition of candidate clones by ic-ELISA were done with nanobody-GIII fusion protein (Fig. S3). Clones showing the high binding activity against coating antigen and good inhibition in the presence of 500 ng/mL 2,4-D were selected and sequenced. As shown in Fig. 3, unique nanobody clones with different protein sequences were

Table 2
Cross-reactivity of the rabbit pAb #1518 and nanobody NB3-9 against 2,4-D analogs.

Compound	Cross Reactivity (%)		Compound	Cross Reactivity (%)	
	pAb #1518	Nanobody NB3-9		pAb #1518	Nanobody NB3-9
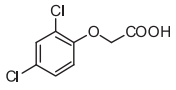 2,4-D	100	100	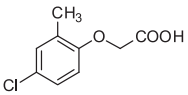 MCPA	11.3	4.5
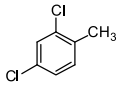 2,4-Dichlorotoluene	<1	<1	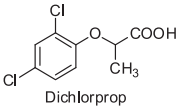 Dichlorprop	4.7	0.8
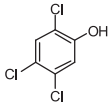 2,4-Dichlorophenol	<1	<1	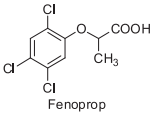 Fenoprop	9.9	0.9
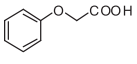 phenoxyacetic acid	<1	<1	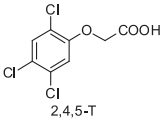 2,4,5-T	156.6	5.1
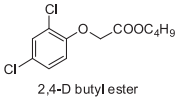 2,4-D butyl ester	35.4	1.8	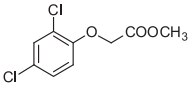 2,4-D methyl ester	38.8	1.5

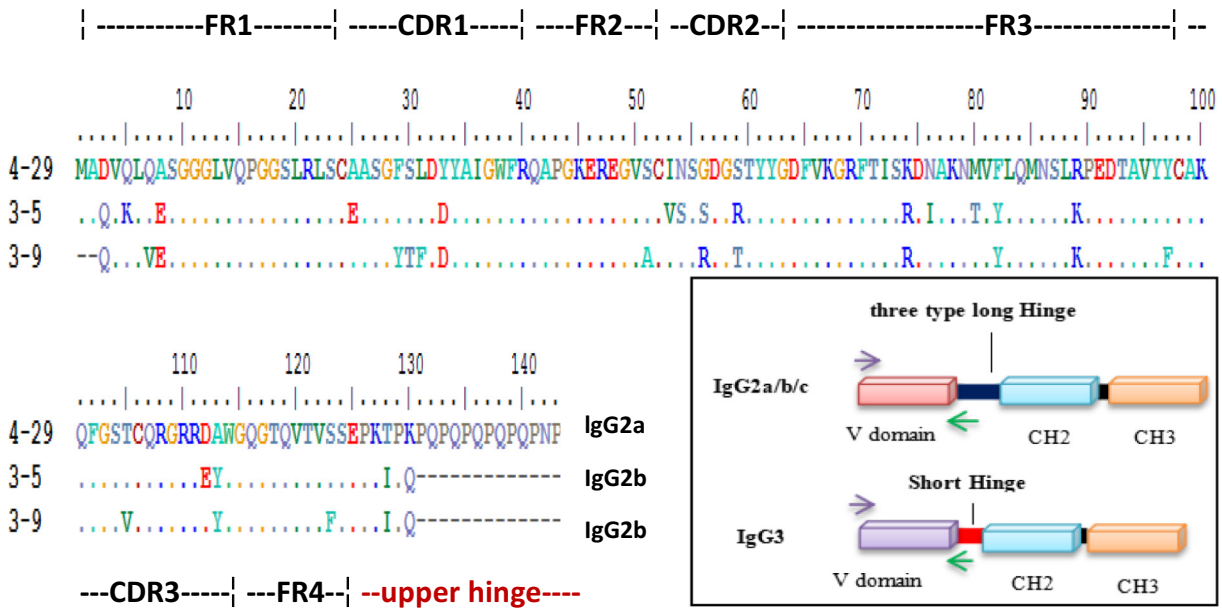

Fig. 3. The positive nanobody candidates isolated from subclass specific phage-display library based on one-step PCR construction strategy (rectangle box). Nanobody's V domain was directly amplified in cloning procedure from FR1 to upper hinge region (including long hinge IgG2a/b/c and short hinge IgG3subclass). The isolated nanobody protein sequence was assigned to different subclass according to the sequence of upper hinge(red). (For interpretation of the references to colour in this figure legend, the reader is referred to the web version of this article.)

identified, with upper hinge tail different from the conventional heavy antibodies. Based on the upper hinge, one of them was classified as IgG2a nanobody, the other two as IgG2b nanobodies.

3.4. Specificity and sensitivity of selected nanobodies

Llama immunization with the confirmed immunogen, monitoring of the heavy chain antibody in serum, and one-step PCR library construction were performed with the ultimate goal to isolate a nanobody with excellent specificity and sensitivity. As shown in Fig. 2b, the selected nanobodies have good sensitivity in the detection of 2,4-D; the best clone NB3-9 had IC_{50} of 29.2 ng/mL among these selected clones. In general, this result indicated that the isolation of a nanobody library was successful. The one-step PCR library construction provided diversity rich enough to isolate positive clones, and the stringent bio-panning in competitive mode guaranteed the eluted clones specifically against 2,4-D.

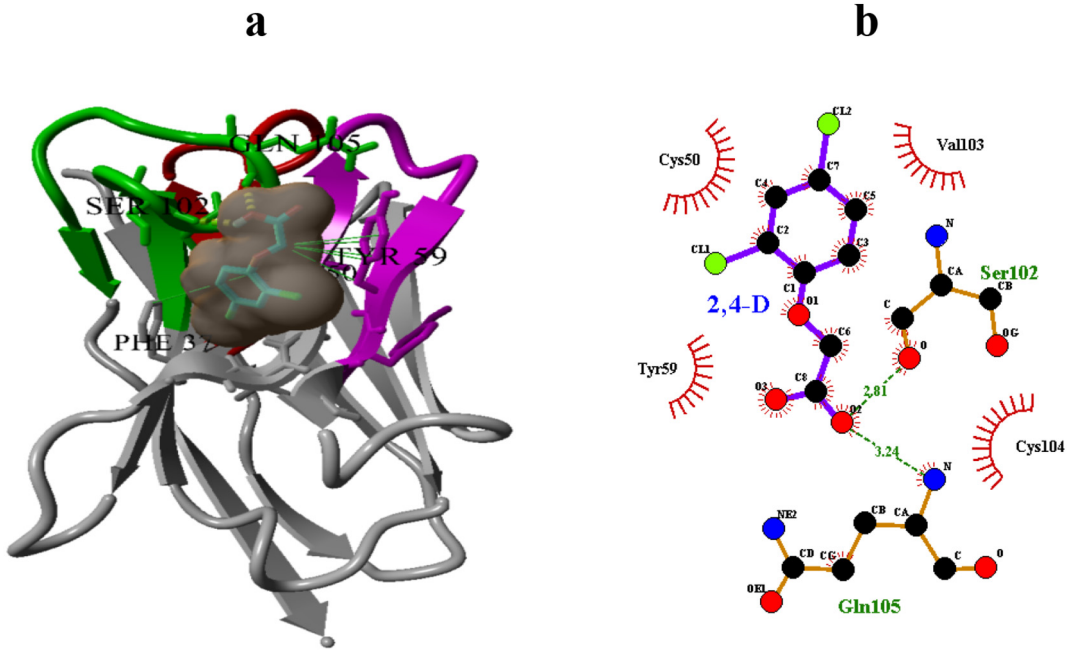

Fig. 4. The recognition mode between NB3–9 and 2,4-D in 3D docking plot(a) and the 2D interaction plot(b). The structure of NB3–9 in ribbon style with three CDR highlighted (CDR1/red, CDR2/purple, CDR3/green) and the structure of 2,4-D in stick style covered by molecular surface. The hydrogen bond was labeled in yellow dotted line, and the hydrophobic interaction was labeled in green line. The distance of hydrogen bond and hydrophobic force of the adjacent residues surrounding 2,4-D was highlighted in the 2D plot. (For interpretation of the references to colour in this figure legend, the reader is referred to the web version of this article.)

The clone NB3-9 was further tested for cross-reactivity with 2,4-D analogs (Table 2). The result showed that the specificity of NB3-9 was improved dramatically. The obvious cross-reactivity against 2,4-D esters was still found in the pAb-based ELISA, but almost no cross-reactivity (CR) with these 2,4-D esters was observed in nanobody-based ELISA. It indicated that the isolated NB3-9 has better specificity than pAb#1518 raised by the same immunogen. In the previous study, pAb-based ELISA has 156.6% CR with 2,4,5-T; this compound is almost the same as 2,4-D except for an extra chlorine group. Surprisingly, only slight cross-reactivity in nanobody-based ELISA was observed for 2,4-D analogs like MCPA, dichlorprop, fenoprop and 2,4,5-T, even though they all have similar structure as 2,4-D. We speculated that nanobodies as the smallest size single-epitope binder could recognize the unique structural features on 2,4-D chemical structure, which is the key factor in distinguishing the 2,4-D analogs.

3.5. The recognition mechanism of nanobody3-9 against 2,4-D

To illuminate the mechanism of interactions between nanobody and 2,4-D, the 3D structure of NB3-9 was constructed by homogenous modeling, and a docking study was conducted by molecular simulation. After searching the PDB database, a crystal structure of camelid derived antibody (PDB:5HGG) with high sequence similarity was purposefully selected as a template to create a homology model. The PROCHECK evaluation results of this model showed that the residues in most favored regions rate were 93.1% (Fig. S4), which indicated that the protein model constructed was a high-quality model. This model was docked with 2,4-D in a simulation box of the possible binding sites surrounding three CDR regions. As shown in Fig. 4a, 2,4-D was deeply buried in the pocket formed by CDR3 and CDR2. The binding pocket of NB3-9 has many interactions with 2,4-D, including 2 hydrogen bonds (yellow, Ser102, and Gln105) and several hydrophobic forces (green, Tyr59, Phe37 and Cys50). Detailed information about the recognition mechanism was shown in 2D plot (Fig. 4b), including the distance of hydrogen bonds on the carboxyl group of 2,4-D structure and the hydrophobic force surrounding the 2,4-D structure. This docking study illuminated the binding pattern of NB3-9 against 2,4-D, which matched the ic-ELISA result in the specificity study to some extent. For example, the 2,4-D butyl ester and the 2,4-D methyl ester have the same chlorophenoxy group as 2,4-D, but are missing the unique free carboxyl group, so they could not form hydrogen bonds with NB3-9. This phenomenon supported our hypothesis in hapten design. Meanwhile, we assumed that the intact structural conformation of 2,4-D also plays a critical role for immuno-recognition. Though MCPA, dichlorprop, fenoprop, and 2,4,5-T have the carboxyl group like 2,4-D, they all have different functional groups on the chlorophenoxy group near the carboxyl group. The docking study demonstrated that the extreme specificity of the nanobody NB3-9 against 2,4-D was attributed by the hydrophobic force surrounding entire conformation features of 2,4-D chemical structure, especially the chlorophenoxy group. Though other 2,4-D analogs have high similar structure as 2,4-D, the nanobody was still able to discriminate the tiny structural differences between them. Overall, the high selective NB3-9 could distinguish 2,4-D from many other analogs, which will improve the performance of the nanobody-based immunoassay when applied for the real environmental sample.

3.6. One-step FLEIA/ELEIA based on nanobody-alkaline phosphatase fusion

As reported previously, nanobodies fused with alkaline phosphatase (AP) as immuno reagents have shown significant potential in one-step immunoassays for the detection of small molecules like Triazophos (Wang et al., 2019)and 3-phenoxybenzoic acid (Huo et al., 2018). Since the anti-2,4-D nanobody NB3-9 is a recombinant binder, it is easy to construct the nanobody-AP fusion plasmid by molecular cloning. As shown in Fig. S5, NB3-9 fused with AP was easily expressed in the periplasmic space of *E.coli*, with an expected size of 65 kDa determined by SDS-PAGE. In this study, both colorimetric and fluorometric analyses were applied to assess the potency of the nanobody–AP fusion. The one-step ELISA based on the nanobody-AP fusion has an IC_{50} of 11.6 ng/mL (Fig. 5), which is 3 times lower than that of the classic two-step ELISA based on parental nanobody NB3-9 (IC_{50} of 29.2 ng/mL). In addition, because of strong signal amplification with the BBTP substrate, it was more sensitive to exploit enzyme catalytic activity of the nanobody-AP fusion in fluorometric mode than the colorimetric mode. The concentration of coating antigen could be decreased from 1 μg/mL in the colorimetric assay to 0.05 μg/mL in the fluorometric assay. Generally, the less of immunogen reagent concentration leads to better inhibition by the free analyte in competitive assay mode. As shown in Fig. 5, The standard curve for both one-step Nanobody-AP assay were fitted in good quality ($R^2 > 0.99$), the working range are 0.4–8.6 ng/mL for FLEIA and 2.7–49.6 ng/mL for ELISA, respectively. It can be concluded that the developed FLEIA has 5 times better sensitivity than the one-step ELISA by comparison the IC_{50} of 1.9 ng/mL(FLEIA) with 11.6 ng/mL(ELISA).

3.7. Validation of FELIA in spiked and real water sample

Usually, the 2,4-D selective immunoassay was developed and applied for the detection 2,4-D residues in the drinking water (Wilmer et al., 1997). However, the extensive use of 2,4-D herbicide in 2,4-D resistant crop fields needs regular monitoring of the contamination of 2,4-D in surface and groundwater. The environmental water might have complex matrix (Oldfield, 2014; Sun and Liu, 2018), which is one of the major challenges in immunoassay development. Usually, the matrix effects can be reduced by sample dilution(Sykorova et al., 2018). In our work, the environmental water samples with 1/2 and 1/5 fold dilution in the PBS buffer and the undiluted water were tested in FLEIA for assessment of matrix effect. After 5-fold dilution, the standard curve of river water and lake water overlapped completely with that of the PBS buffer (Fig. S6). According to the guidelines of WHO (WHO, 2011), 2,4-D residual in drinking water should be less than 30 ng/mL, the detection of limit (LOD) of our developed FLEIA met this requirement since LOD was calculated by IC_{10} plus 5-fold dilution factor as 1.2 ng/mL for water sample. To validate the reliability of FLEIA, the method was performed to determine 2,4-D in the spiked water samples, including Solano river and Berryessa lake water in Sacramento, CA, US. The 2,4-D spiked with three different concentrations of 2,4-D (3, 10, and 30 ng/mL) were analyzed by FLEIA, the average recoveries for FLEIA ranged from 92.8 to 95.7% (Table 3). Also, the developed FLEIA was applied for the detection of environmental surface water samples provided by the department of pesticide regulation in California state

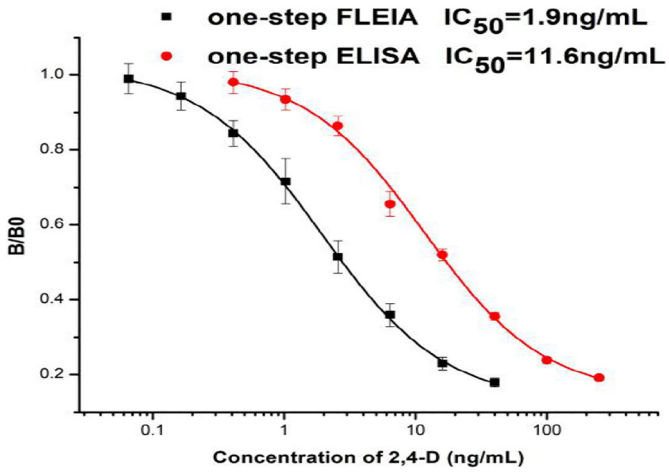

Fig. 5. Standard curves of one-step FLEIA based on BBTP fluorogenic substrate and one-step ELISA based on pNPP chromogenic substrate.

Table 3
Recovery of spiked water samples determined by FLEIA(n = 3).

Spiked 2,4-D (ng/mL)		Detected 2–4-D (ng/mL) Average ± SD(n = 3)			Recovery (%)
	3	2.87	±	0.25	95.7
	10	9.35	±	0.31	93.5
Lake water	30	28.67	±	0.26	95.6
	3	2.83	±	0.36	94.3
	10	9.36	±	0.24	93.6
River water	30	27.83	±	0.31	92.8

and validated by LC-MS/MS. The ppb levels (1.3 and 1.8 ng/mL) of trace 2,4-D in environmental waters were consistent by FLEIA and LC-MS/MS (Table 4).

4. Conclusions

Recently, the sale of herbicide Dicamba was blocked by EPA in US (Bomgardner, 2020), which will likely lead to a dramatic increase in the use of 2,4-D to exploit the widely used 2,4-D resistant crop. Immunoassay is a rapid and high-throughput tool for monitoring the contamination of 2,4-D herbicide in the environment. The performance of immunoassay largely relies on the quality of antibodies, whose sensitivity and specificity were difficult to control and optimize during the traditional procedure of antibody generation. Taking herbicide 2,4-D as a model analyte, we generated a novel nanobody against 2,4-D by a step-wise strategy, including consecutive steps form hapten design, serum assessment to one-step phage-display library construction. The isolated nanobody NB3-9 exhibited better specificity against 2,4-D than the pAb#1518, with only insignificant cross-reactivity to 2,4-D analogs. Finally, a rapid and sensitive FLEIA based on a nanobody-AP fusion was successfully developed. This one-step FLEIA had excellent sensitivity and accuracy for the detection of 2,4-D contamination in the environmental water samples. Overall, we present a reliable workflow to obtain a high selective anti-hapten nanobody, which is an efficient way to develop a nanobody-based immunoassay for monitoring the pollutant in the environment.

CRediT authorship contribution statement

Zhen-Feng Li, Jie-Xian Dong: Methodology, Writing-Original draft preparation.Natalia Vasylieva, Yong-Liang Cui, De-Bin Wan: Sample preparation and Data analysis.Jing-Qian Huo, Dong-Chen Yang: Assay development and Validation. Xiu-De Hua, Shirley J. Gee: Reviewing and Editing. Bruce D. Hammock: Conceptualization and Supervision.

Author contributions

Zhen-Feng Li and Jie-Xian Dong contributed equally to this work.

Declaration of competing interest

The authors declare that they have no known competing financial interests or personal relationships that could have appeared to influence the work reported in this paper.

Table 4
Detection of real environmental water samples (n = 3).

Water sample	LC/MS(ng/mL)	FLEIA(ng/mL)
NO.2077	0.3 ± 0.08	ND.
NO.4271	1.7 ± 0.25	1.8 ± 0.13
NO.4121	1.2 ± 0.23	1.3 ± 0.14

Acknowledgments

The authors thank the support of the National Institute of Environmental Health Science Superfund Research Program (P42ES004699) and National Institute of Health RIVER Award (R35 ES030443-01). This work was partial supported by the National Academy of Sciences and USAID (NAS, Sub-Award No. 2000009144). Any opinions, findings, conclusions, or recommendations expressed in such article are those of the authors alone, and do not necessarily reflect the views of USAID or NAS."

Appendix A. Supplementary data

Chemicals and reagent; synthesis of hapten; preparation of immunogen and coating antigen; immunization and antiserum assessment; library construction and nanobody screening; the development of FLEIA/ELISA based on nanobody-AP fusion. Supplementary data to this article can be found online at doi:10.1016/j.scitotenv.2020.141950

References

Arbabi Ghahroudi, M., Desmyter, A., Wyns, L., Hamers, R., Muyldermans, S., 1997. Selection and identification of single domain antibody fragments from camel heavy-chain antibodies. FEBS Lett. 414, 521–526.

Bever, C.S., Dong, J.-X., Vasylieva, N., Barnych, B., Cui, Y., Xu, Z.-L., et al., 2016. VHH antibodies: emerging reagents for the analysis of environmental chemicals. Anal. Bioanal. Chem. 408, 5985–6002.

Bomgardner, M.M., 2020. EPA says farmers can use dicamba through July: agency moves to help farmers after court rules herbicide should not have been registered. Chem. Eng. News 98, 15.

Burns, C.J., Swaen, G.M.H., 2012. Review of 2,4-dichlorophenoxyacetic acid (2,4-D) biomonitoring and epidemiology. Crit. Rev. Toxicol. 42, 768–786.

Cevallos-Cedeno, R.E., Agullo, C., Abad-Somovilla, A., Abad-Fuentes, A., Mercader, J.V., 2018. Hapten design and antibody generation for immunoanalysis of spirotetramat and spirotetramat-enol. ACS Omega 3, 11950–11957.

Daley, L.P., Gagliardo, L.F., Duffy, M.S., Smith, M.C., Appleton, J.A., 2005. Application of monoclonal antibodies in functional and comparative investigations of heavy-chain immunoglobulins in new world camelids. Clin. Diagn. Lab. Immunol. 12, 380–386.

Egan, J.F., Maxwell, B.D., Mortensen, D.A., Ryan, M.R., Smith, R.G., 2011. 2,4-Dichlorophenoxyacetic acid (2,4-D)–resistant crops and the potential for evolution of 2,4-D–resistant weeds. Proc. Natl. Acad. Sci. U. S. A. 108, E37.

Feng, X.L., Zhang, G., Chin, L.K., Liu, A.Q., Liedberg, B., 2017. Highly sensitive, label-free detection of 2,4-dichlorophenoxyacetic acid using an optofluidic chip. Acs Sensors 2, 955–960.

Forli, S., Huey, R., Pique, M.E., Sanner, M.F., Goodsell, D.S., Olson, A.J., 2016. Computational protein–ligand docking and virtual drug screening with the AutoDock suite. Nat. Protoc. 11, 905–919.

Franek, M., Kolar, V., Granatova, M., Nevorankova, Z., 1994. Monoclonal Elisa for 2,4-dichlorophenoxyacetic acid - characterization of antibodies and assay optimization. J. Agric. Food Chem. 42, 1369–1374.

Gamhewage, M., Farenhorst, A., Sheedy, C., 2019. Phenoxy herbicides' interactions with river bottom sediments. J. Soils Sediments 19, 3620–3630.

Gerdes, M., Meusel, M., Spener, F., 1997. Development of a displacement immunoassay by exploiting cross-reactivity of a monoclonal antibody. Anal. Biochem. 252, 198–204.

Griffin, L.M., Snowden, J.R., Lawson, A.D., Wernery, U., Kinne, J., Baker, T.S., 2014. Analysis of heavy and light chain sequences of conventional camelid antibodies from Camelus dromedarius and Camelus bactrianus species. J. Immunol. Methods 405, 35–46.

Hamers-Casterman, C., Atarhouch, T., Muyldermans, S., Robinson, G., Hammers, C., Songa, E.B., et al., 1993. Naturally occurring antibodies devoid of light chains. Nature 363, 446–448.

Hassanzadeh-Ghassabeh, G., Devoogdt, N., De Pauw, P., Vincke, C., Muyldermans, S., 2013. Nanobodies and their potential applications. Nanomedicine (Lond) 8, 1013–1026.

He, T., Zhu, J., Nie, Y., Hu, R., Wang, T., Li, P., et al., 2018. Nanobody technology for mycotoxin detection in the field of food safety: current status and prospects. Toxins (Basel) 10.

Huo, J., Li, Z., Wan, D., Li, D., Qi, M., Barnych, B., et al., 2018. Development of a highly sensitive direct competitive fluorescence enzyme immunoassay based on a nanobody-alkaline phosphatase fusion protein for detection of 3-phenoxybenzoic acid in urine. J. Agric. Food Chem. 66, 11284–11290.

Kastelic, D., Frkovic-Grazio, S., Baty, D., Truan, G., Komel, R., Pompon, D., 2009. A single-step procedure of recombinant library construction for the selection of efficiently produced llama VH binders directed against cancer markers. J. Immunol. Methods 350, 54–62.

Kaur, J., Boro, R.C., Wangoo, N., Singh, K.R., Suri, C.R., 2008. Direct hapten coated immunoassay format for the detection of atrazine and 2,4-dichlorophenoxyacetic acid herbicides. Anal. Chim. Acta 607, 92–99.

Khodabakhsh, F., Behdani, M., Rami, A., Kazemi-Lomedasht, F., 2018. Single-domain antibodies or nanobodies: a class of next-generation antibodies. Int. Rev. Immunol. 37, 316–322.

Kim, H.J., McCoy, M.R., Majkova, Z., Dechant, J.E., Gee, S.J., Tabares-da Rosa, S., et al., 2012. Isolation of alpaca anti-hapten heavy chain single domain antibodies for development of sensitive immunoassay. Anal. Chem. 84, 1165–1171.

Krieger, E., Koraimann, G., Vriend, G., 2002. Increasing the Precision of Comparative Models with YASARA NOVA—A Self-Parameterizing Force Field. vol. 47 pp. 393–402.

Laskowski, R.A., MacArthur, M.W., Moss, D.S., Thornton, J.M., 1993. PROCHECK: a program to check the stereochemical quality of protein structures. J. Appl. Crystallogr. 26, 283–291.

Lawruk TH, C.; Fleeker, J.; Hall, J.; Herzog, D.; Rubio, F. Quantification of 2, 4-D and related chlorophenoxy herbicides by a magnetic particle-based ELISA. Bull. Environ. Contam. Toxicol. 1994; 52.

van der Linden, R., de Geus, B., Stok, W., Bos, W., van Wassenaar, D., Verrips, T., et al., 2000. Induction of immune responses and molecular cloning of the heavy chain antibody repertoire of Lama glama. J. Immunol. Methods 240, 185–195.

Matuszczyk, G., Knopp, D., Nießner, RjFJoAC, 1996. Development of an ELISA for 2,4-D: Characterization of Two Polyclonal Antisera. vol. 354 pp. 41–47.

Mi, J., Dong, X., Zhang, X., Li, C., Wang, J., Mujtaba, M.G., et al., 2019. Novel hapten design, antibody recognition mechanism study, and a highly sensitive immunoassay for diethylstilbestrol in shrimp. Anal. Bioanal. Chem. 411, 5255–5265.

Mohammadnia, M., Heydari, R., Sohrabi, M.R., 2019. Determination of 2,4-Dichlorophenoxyacetic acid in food and water samples using a modified graphene oxide sorbent and high-performance liquid chromatography. J. Environ. Sci. Health B 1–8.

Mu, H., Lei, H., Wang, B., Xu, Z., Zhang, C., Ling, L., et al., 2014. Molecular modeling application on hapten epitope prediction: an enantioselective immunoassay for ofloxacin optical isomers. J. Agric. Food Chem. 62, 7804–7812.

Oldfield, P.R., 2014. Understanding the matrix effect in immunoassays. Bioanalysis 6, 1425–1427.

Pardon, E., Laeremans, T., Triest, S., Rasmussen, S.G., Wohlkonig, A., Ruf, A., et al., 2014. A general protocol for the generation of Nanobodies for structural biology. Nat. Protoc. 9, 674–693.

Seebunrueng, K., Phosiri, P., Apitanagotinon, R., Srijaranai, S., 2020. A new environment-friendly supramolecular solvent-based liquid phase microextraction coupled to high performance liquid chromatography for simultaneous determination of six phenoxy acid herbicides in water and rice samples. Microchem. J. 152, 104418.

Sun, J., Liu, Y., 2018. Matrix effect study and immunoassay detection using electrolyte-gated graphene biosensor. Micromachines (Basel) 9.

Sykorova, S., Fojtikova, L., Kuchar, M., Miksatkova, P., Karamonova, L., Fukal, L., et al., 2018. Sensitive enzyme immunoassay for screening methandienone in dietary supplements. Food Addit Contam Part A Chem Anal Control Expo Risk Assess 35, 1653–1661.

Tabares-da Rosa, S., Rossotti, M., Carleiza, C., Carrion, F., Pritsch, O., Ahn, K.C., et al., 2011. Competitive selection from single domain antibody libraries allows isolation of high-affinity antihapten antibodies that are not favored in the llama immune response. Anal. Chem. 83, 7213–7220.

Teixeira, M.C., Duque, P., Sa-Correia, I., 2007. Environmental genomics: mechanistic insights into toxicity of and resistance to the herbicide 2,4-D. Trends Biotechnol. 25, 363–370.

Tillib, S.V., Vyatchanin, A.S., Muyldermans, S., 2014. Molecular analysis of heavy chain-only antibodies of Camelus bactrianus. Biochemistry (Mosc) 79, 1382–1390.

Togtema, M., Hussack, G., Dayer, G., Teghtmeyer, M.R., Raphael, S., Tanha, J., et al., 2019. Single-domain antibodies represent novel alternatives to monoclonal antibodies as targeting agents against the human papillomavirus 16 E6 protein. Int. J. Mol. Sci. 20.

Wang, J., Bever, C.R., Majkova, Z., Dechant, J.E., Yang, J., Gee, S.J., et al., 2014. Heterologous antigen selection of camelid heavy chain single domain antibodies against tetrabromobisphenol A. Anal. Chem. 86, 8296–8302.

Wang, K., Liu, Z., Ding, G., Li, J., Vasylieva, N., Li, Q.X., et al., 2019. Development of a one-step immunoassay for triazophos using camel single-domain antibody-alkaline phosphatase fusion protein. Anal. Bioanal. Chem. 411, 1287–1295.

WHO, 2011. guidelines for drinking water. https://www.who.int/water_sanitation_health/publications/2011/dwq_guidelines/en/.

Wilmer, M., Trau, D., Renneberg, R., Spener, F., 1997. Amperometric immunosensor for the detection of 2,4-dichlorophenoxyacetic acid (2,4-D) in water. Anal. Lett. 30, 515–525.

Zuanazzi, N.R., Ghisi, N.C., Oliveira, E.C., 2020. Analysis of global trends and gaps for studies about 2,4-D herbicide toxicity: a scientometric review. Chemosphere 241, 125016.